National Research Council Canada
Conseil national de recherches Canada

TURBULENT BOUNDARY LAYER SOLUTION FOR TWO-DIMENSIONAL COMPRESSIBLE FLOW USING MIXING LENGTH AND K-ε TURBULENCE MODELS

by

M. Khalid

Institute for Aerospace Research

OTTAWA
NOVEMBER 1990

AERONAUTICAL NOTE
IAR-AN-
NRC NO. 30

Canada

UNLIMITED
UNCLASSIFIED

91-02915/

INSTITUTE FOR AEROSPACE RESEARCH

SCIENTIFIC AND TECHNICAL PUBLICATIONS

AERONAUTICAL REPORTS

Aeronautical Reports (LR): Scientific and technical information pertaining to aeronautics considered important, complete, and a lasting contribution to existing knowledge.

Mechanical Engineering Reports (MS): Scientific and technical information pertaining to investigations outside aeronautics considered important, complete, and a lasting contribution to existing knowledge.

AERONAUTICAL NOTES (AN): Information less broad in scope but nevertheless of importance as a contribution to existing knowledge.

LABORATORY TECHNICAL REPORTS (LTR): Information receiving limited distribution because of preliminary data, security classification, proprietary, or other reasons.

Details on the availability of these publications may be obtained from:

Graphics Section,
National Research Council Canada,
Institute for Aerospace Research,
Bldg. M-16, Room 204,
Montreal Road,
Ottawa, Ontario
K1A 0R6

INSTITUT DE RECHERCHE AÉROSPATIALE

PUBLICATIONS SCIENTIFIQUES ET TECHNIQUES

RAPPORTS D'AÉRONAUTIQUE

Rapports d'aéronautique (LR): Informations scientifiques et techniques touchant l'aéronautique jugées importantes, complètes et durables en termes de contribution aux connaissances actuelles.

Rapports de génie mécanique (MS): Informations scientifiques et techniques sur la recherche externe à l'aéronautique jugées importantes, complètes et durables en termes de contribution aux connaissances actuelles.

CAHIERS D'AÉRONAUTIQUE (AN): Informations de moindre portée mais importantes en termes d'accroissement des connaissances.

RAPPORTS TECHNIQUES DE LABORATOIRE (LTR): Informations peu disséminées pour des raisons d'usage secret, de droit de propriété ou autres ou parce qu'elles constituent des données préliminaires.

Les publications ci-dessus peuvent être obtenues à l'adresse suivante:

Section des graphiques,
Conseil national de recherches Canada,
Institut de recherche aérospatiale,
Im. M-16, pièce 204,
Chemin de Montréal,
Ottawa (Ontario)
K1A 0R6

UNLIMITED
UNCLASSIFIED

TURBULENT BOUNDARY LAYER SOLUTION FOR TWO-DIMENSIONAL COMPRESSIBLE FLOW USING MIXING LENGTH AND K–ε TURBULENCE MODELS

RÉSOLUTION DU PROBLÈME DES COUCHES LIMITES TURBULENTES COMPRESSIBLES BIDIMENSIONNELLES AU MOYEN DES MODÈLES DE TURBULENCE K-ε ET DE LONGUEUR DE MÉLANGE ACCRUE

by/par

M. Khalid

Institute for Aerospace Research

OTTAWA
NOVEMBER 1990

AERONAUTICAL NOTE
IAR-AN-69
NRC NO. 32135

Y. Y. Chan, Head/Chef
High Speed Aerodynamics Laboratory
Laboratoire d'aérodynamique à hautes vitesses

G.F. Marsters
Director General
Le directeur général

SUMMARY

The continuity, momentum and energy equations for two-dimensional compressible turublent boundary layers are solved using the k-ε turbulence model and the extended mixing length approach to calculate the shear stress terms. The finite difference equations are set up applying Keller's box scheme and the resulting tridiagonal matrix system is solved by the block elimination method. Newton's iteration procedure is used to converge the solution. Results obtained from computations showed only slight difference between the two methods. Both methods showed satisfactory agreement with experimental data for test cases.

RÉSUMÉ

Les équations de continuité, de quantité de mouvement et d'énergie pour des couches limites turbulentes compressibles bidimensionnelles sont résolues au moyen du modèle de turbulence K-ε et de la méthode de la longueur de mélange accrue (1) pour calculer les termes de contrainte de cisaillement. Les équations aux différences finies sont établies par l'application du modèle de la boîte de Keller, et le système matriciel tridiagonal résultant est résolu par la méthode d'élimination par blocks. La méthode d'itération de Newton est utilisé pour converger vers la solution. Les résultats obtenus des calculs n'ont révélé que de faibles écarts entre les deux méthodes, lesquelles sont en bon accord avec les données expérimentales pour les cas étudiés.

Symbols

b	$\rho u/\rho_e u_e(1+\nu_t/\nu)$
c	reference length
C	$\rho u/\rho_e u_e$
c_k	0.33, c_1 = 1.44, c_2 = 1.90 and c_3 = 4.44
c_μ	0.09
c_f	skin friction coefficient $(\tau_w/(1/2\rho_e u_e^2))$
d	$Cu_e^2/H_e(1-1/Pr+\nu_t/\nu(1-1/Pr_t))$
e	$C/Pr(1+Pr/Pr_t\ (\nu_t/\nu))$
g	H/H_e
H	enthalpy (c_pT)
m_1	$1/2(1 + m_2 + (x/\rho_e u_e)d(\rho_e\mu_e)/dx)$
m_2	$x/u_e(du_e/dx)$
k	turbulent kinetic energy
k_t	eddy conductivity
u , v	longitudinal and lateral components of flow velocity. in finite difference approximation of equations in first order they refer to normal gradients, i.e u=f' and v=u'.
u_τ	$\sqrt{\tau_w}/_\rho$
Re	Reynolds number
R_x	Reynolds number based on the chordwise distance x from leading edge
R_θ	Reynolds number based on the momentum thickness, θ
Pr	Prandtl number $\mu c_p/k$ where k is the thermal conductivity constant
T	temperature
x, y	Cartesian coordinates
y^+	yu_τ/θ
y_0	location where u/u_e =0.995
δ	boundary layer thickness
δf, δF..	incremental amounts used in Newton's iteration procedure
δ^*	displacement thickness
θ	momentum thickness
τ	shear stress $(\mu_1 + \mu_t)\partial u/\partial y$
ρ	density
ϵ	dissipation rate
ν	kinematic viscosity μ/ρ
η	transformed lateral coordinate
ψ	transformed stream function
λ	$c_\mu k^2/\epsilon.(c\rho^2 u_e/\rho^2{}_e\nu_e)$

Subscripts

t	turbulent
w, 1	wall conditions
e	boundary layer edge conditions
l	laminar
∞	free stram conditions

Table of Contents

		Page
	Summary	(iii)
	Symbols	(iv)
	List of Figures	(vi)
1.	Introduction	1
2.	Background of Turbulence Models	1
3.	The Boundary Layer Equations	3
4.	Extended Mixing Length (Cebeci-Smith) Method	8
5.	The K-ϵ Turbulence Model	9
6.	Discussion of Results	13
7.	Conclusions	15
	References	15

List of Figures

		Page
1.	Grid rectangle for the finite difference scheme	17
2.	Skin friction coefficient C_f versus axial distance	18
3.	Velocity U/U_e and shear stress τ profiles across boundary layer	19
4.	Velocity U/U_e and shear stress τ profiles across boundary layer	20
5.	Velocity U/U_e and shear stress τ profiles across boundary layer	21
6.	Skin friction coefficient C_f versus x/c	22
7.	Skin friction coefficient C_f versus x/c	23
8.	Displacement thickness δ^* and form parameter H versus x/c	24
9.	Velocity U/U_e and shear stress τ profiles across boundary layer	25
10.	Velocity U/U_e and shear stress τ profiles across boundary layer	26
11.	Velocity U/U_e and shear stress τ profiles across boundary layer	27
12.	Velocity U/U_e and shear stress τ profiles across boundary layer	28
13.	Velocity U/U_e and shear stress τ profiles across boundary layer	29
14.	Displacement thickness δ^* versus x/c	30
15.	Momentum thickness θ versus x/c	31

TURBULENT BOUNDARY LAYER SOLUTION FOR TWO-DIMENSIONAL COMPRESSIBLE FLOW USING MIXING LENGTH AND K-ϵ TURBULENCE MODELS

1. Introduction

This report contains outlines of two methods for calculating the boundary layer characteristics. The two methods, the extended mixing length approach due to Cebeci-Smith [1] and the k-ϵ method first developed by Jones and Launder [2] have been applied, elsewhere, to a variety of fluid dynamics problems to model turbulence. Here, at the Institute for Aerospace Research (IAR) we are in the process of developing our own 2 D Euler codes with the ultimate objective of an inhouse 3 D Navier Stokes capability. We investigated the efficiency and the convenience of usage of the two methods for providing the turbulence coupling in our codes.

The report describes how the two models are individually incorporated in the finite difference scheme of the overall boundary layer equations. For the mixing length approach the method of solution remains the same as the one given in Ref [1], however for the use of k-ϵ model the approach differs from the one in Ref [3] and [4] in that momentum equation is not reintroduced to be solved along with the k-ϵ set of equations. The two methods were applied to a number of cases selected from the Stanford Conference of 1980-1981 [5] . The comparison of computed results against experiments are provided.

2. Background of Turbulence Models

A number of turbulence models have been developed over the last two decades which successfully model the shear stress terms of the boundary layer equations. The classic amongst these is the Prandtl's mixing length model [6] which is the forerunner of today's algebraic models such as those developed by Patankar-Spalding [7], Cebeci-Smith [1] , Launder-Pridden [8], and Kays-Moffat [9].

The mixing length concept is based on a simple relationship which relates the turbulent eddy viscosity in the inner region of the boundary layer to a mixing length and a mean velocity gradient,i.e.

$$\nu_t = l^2 |\partial u/\partial y| \qquad (1)$$

where

$$l=\kappa y.$$

κ here is the von Karman constant having a value of about 0.4 to 0.41, or when using Van Driest's [10] extended relationship,

$$l=\kappa y(1-\exp(-y^{+}/A_0)) \tag{3}$$

when the laminar sublayer is included. The constant A_0 has a value of $\approx$ 26 and $y^{+}=yu_{\tau}/\theta$ ($u_{\tau}=\sqrt{\tau_w/\rho}$). Indeed van Driest's extended relationship actually set the stage for the algebraic models which were to follow.

In some of the earlier models, based on the mixing length concept (Ref 1 and 6 to 10), the mixing length of the outer region of the boundary layer was correlated to the local thickness of the boundary layer which seemed to work well for flat plate type flows with moderate pressure gradients. They were not as accurate for flow with large adverse pressure gradients.

Some later turbulence models such as the ones by McDonald and Camarata [11], and Bradshaw et al [12] addressed this shortcoming by accounting for the mixing length using an integral form of the turbulence kinetic energy equation. In Reference 12 , use of an experimental observation, $u'v'/k \approx 0.3$ is made to express the turbulence kinetic energy equation as an eddy stress equation with the diffusion term and the mixing length being proportional to simple functions of y/δ.

Using the turbulence kinetic energy equation, Chan [13], adopted a differential approach based on finite difference formulation rather than the above integral solutions for successful application on compressible turbulent flows with pressure gradients.

The Baldwin and Lomax method [14] uses a mean vorticity gradient rather than a mean velocity gradient to express the eddy viscosity in the outer region. Lilley [15] in 1960 had used the concept of a virtual eddy viscosity in the outer regions of boundary layer instead of the traditional mixing length approach to show that turbulent boundary layer equation can be solved approximately to obtain a velocity distribution. The compatibility

condition of his solution $(\frac{u_\tau \delta}{\nu_t} = cons.)$ agreed well with Townsend's equilibrium condition [16] .

In recent years computational methods for turbulence modelling have gained more acceptance. The classic amongst these is the Reynolds stress model by Hanjalic and Launder [17] where the differential transport equations for shear stress, the turbulence kinetic energy (k) and the dissipation rate (ϵ) are solved rather than the algebraic equations to effect closure. Another method which has gained increased popularity is the k-ϵ model introduced by Jones and Launder [2] in 1972 . As the name suggests, the method entails the solution of the k and the ϵ equations and the eddy viscosity can then be evaluated from the relationship

$$\nu_t = c_\mu \frac{k^2}{\epsilon} .$$

3. The Boundary Layer Equations

The governing boundary layer equations for two dimensional compressible turbulent flows are:

$$\frac{\partial}{\partial x}(\rho u) + \frac{\partial}{\partial y}(\rho v) = 0 \qquad (4)$$

$$\rho u \frac{\partial u}{\partial x} + \overline{\rho v} \frac{\partial u}{\partial y} = -\frac{dp}{dx} + \frac{\partial}{\partial y}(\mu \frac{\partial u}{\partial y} - \rho \overline{u'v'}) \qquad (5)$$

$$\rho u \frac{\partial H}{\partial x} + \overline{\rho v} \frac{\partial H}{\partial y} = \frac{\partial}{\partial y}[k_t \frac{\partial T}{\partial y} - c_p \rho \overline{T'v'} + u(\mu \frac{\partial u}{\partial y} - \rho \overline{u'v'})] \qquad (6)$$

As in References [1] and [18] and by introducing the eddy viscosity ν_t and the eddy conductivity k_t, with turbulent Prandtl number defined as $Pr_t = \mu c_p / k_t$ we have:

$$-\overline{u'v'} = \nu_t \frac{\partial u}{\partial y}, \qquad -\overline{T'v'} = \frac{\nu_t}{Pr_t} \frac{\partial T}{\partial y} \qquad (7)$$

together with the relationships $-dp/dx=\rho_e u_e(du_e/dx)$.
The boundary conditions used in theses equations are:

$$\begin{aligned} &y=0,\ v = v_w(x),\ u = 0,\ H = H_w(x) \text{ or } \partial H/\partial y = -c_{pw}q_w/k_{tw} \\ &y=\delta,\ u = u_e(x),\ \text{and } H = H_e \end{aligned} \qquad (8)$$

One may rewrite the above momentum and energy equations in terms of a stream function ψ, which satisfies the continuity equation such that:

$$\rho u=\frac{\partial \psi}{\partial y}, \qquad \overline{\rho v}=-\frac{\partial \psi}{\partial x}. \qquad (9)$$

Applying a compressibility transformation to the lateral coordinate y we get;

$$d\eta=\sqrt{\frac{u_e}{\nu_e x}}\frac{\rho}{\rho_e}dy, \qquad (10a)$$

and a similarity transformation to the stream function ψ,

$$\psi(x,y)=\sqrt{\rho_e \mu_e u_e x}\, f(x,\eta), \qquad (10b)$$

enables the transformed momentum and energy equations (as derived in Reference 18) to be written in first order as:

$$bG'+m_1 fG+m_2(C-F^2)=x\left(F\frac{\partial F}{\partial x}-G\frac{\partial f}{\partial x}\right) \qquad (11)$$

$$(eQ+dFG)'+m_1 fQ=x\left(F\frac{\partial g}{\partial x}-Q\frac{\partial f}{\partial x}\right), \qquad (12)$$

where

$$f'=F \qquad (13)$$

$$F'=G \qquad (14)$$

$$g' = Q \tag{15}$$

$$b = \frac{\rho u}{\rho_e u_e}\left(1 + \frac{\nu_t}{\nu}\right), \quad c = \frac{\rho u}{\rho_e u_e}, \tag{16}$$

$$d = \frac{C u_e^2}{H_e}\left(1 - \frac{1}{Pr} + \frac{\nu_t}{\nu}\left(1 - \frac{1}{Pr_t}\right)\right), \quad e = \frac{C}{Pr}\left(1 + \frac{Pr}{Pr_t}\left(\frac{\nu_t}{\nu}\right)\right), \quad g = \frac{H}{H_e} \tag{17}$$

$$m_1 = \frac{1}{2}\left(1 + m_2 + \frac{x}{\rho_e u_e}\frac{d(\rho_e \mu_e)}{dx}\right), \quad m_2 = \frac{x}{u_e}\frac{du_e}{dx} \tag{18}$$

The boundary conditions in transformed coordinates system are:

$$\eta = 0, \qquad f = \frac{1}{\sqrt{\rho_e \mu_e u_e x}}\int_{x1}^{x2} \rho_w v_w dx, \quad g = g_w, \quad or \quad Q = Q_w \tag{19}$$

if transpiration velocity v_w is 0, then f=0 at the wall. At the edge of the boundary layer we have;

$$\eta = 1, \quad F = 1 \quad and \quad g = 1. \tag{20}$$

Equations 11 to 15 consist of a system of first order partial differential equations. Here the symbol prime represents a differentiation with respect to η and the parameters b and d in these equations include viscosity and conductivity terms.

Using an implicit finite difference scheme based on central difference-averaging, the above equation involving variables f,F,G,g and Q are appropriately expressed on the midpoint of the grid rectangle shown in Figure 1. For example at the point $(x^{n-1/2}, \eta)$ and $(x^n, \eta^{j-1/2})$ the function f is given by:

$$f^{n-1/2}{}_j = \frac{1}{2}\left(f^n{}_j + f^{n-1}{}_j\right), \qquad f^n{}_{j-1/2} = \frac{1}{2}\left(f^n{}_j + f^n{}_{j-1}\right) \tag{21}$$

x^n refers to the nth chordwise station.

And similarly a normal gradient of f at the mid-point $(x^{n-1/2}, \eta_{j-1/2})$ is given by the expression:

$$\left(\frac{\partial f}{\partial \eta}\right)^{n-1/2}_{j-1/2} = \frac{\frac{1}{2}\left(f^{n}_{j} + f^{n-1}_{j} - f^{n}_{j-1} - f^{n-1}_{j-1}\right)}{\Delta\eta_j} \qquad (22)$$

where $\Delta\eta_j$ is the incremental step of the jth gridline given by the expression:

$$\eta_j = \Delta\eta_1 \frac{K^{j-1}}{K-1} \qquad (23)$$

The finite differencing on the mid point of the grid rectangle is carried out in an orderly manner. Center the terms first about the midpoint $(x_n, \eta_{j-1/2})$ and then in sequence about the point $(x_{n-1/2}, \eta)$.

To use Keller's box [19] method in combination with Newton's iteration procedure (which has been used by Cebeci and associates in numerous publications to solve non linear equations), it is now required to express the dependent variables f, F, G, g and Q in terms of their respective incremental coefficients ($f + \delta f$, $F + \delta F \ldots$) . For example the equation $f' = F$, in centre difference form at a chordwise station n when expressed in incremental coefficients will have the format:

$$\delta f^{it}_{j} - \delta f^{it}_{j-1} - \frac{\Delta\eta_j}{2}\left(\delta F^{it}_{j} + \delta F^{it}_{j-1}\right) = r^{it}_{j} \qquad (24)$$

where 'it' refers to the iterative value and the right hand side of the equation is given by:

$$r^{it}_{j} = f^{it}_{j} - f^{it}_{j-1} + F^{it}_{j-1/2}\Delta\eta_j \qquad (25)$$

The boundary layer equations can now be expressed as :

$$[L]\Delta = R \qquad (26)$$

Here [L] is a 5 X 5 matrix containing the incremental coefficients of the vector $\Delta(\delta f, \delta F, \delta G, \delta g$ and $\delta Q)$ and R refers to a column vector containing right hand side terms similar to r^{it}_{j} in equation 18.

Applying this procedure on all grid points in the η direction the coefficients form a block tridiagonal matrix. The boundary

conditions at the outer edge of the boundary layer and the wall provide the first and the closing matrices of the tridiagonal matrix system. The complete equation can be written as;

$$\begin{vmatrix} A_0 C_0 & & & & \\ B_1 A_1 C_1 & & & & \\ \cdots\cdots & & & & \\ B_j A_j C_j & & & & \\ \cdots\cdots\cdots & & & & \\ B_{J-1} A_{J-1} C_{J-1} & & & & \\ B_J A_J & & & & \end{vmatrix} \begin{vmatrix} \Delta \end{vmatrix} = \begin{vmatrix} R \end{vmatrix} \qquad (27)$$

It may be noted that when the factorization of matrix [L] is carried out at any j station other than the boundary, the matrix B_j contains the coefficients of the terms like δf_{j-1}, δF_{j-1} .. whereas A_j contains the coefficients of terms like δf_j , δF_j...., . The matrix C_j essentially caters for the terms which involve the information at j+1. The matrices A_0 and A_J completely contain the boundary conditions at the wall and the edge of the boundary layer.

In forward sweep, the initial conditions at the wall,

$$\delta f_0 = 0, \ \delta F = 0, \ \delta g \text{ or } \delta Q = 0 \qquad (28)$$

will determine the contents of the starting anchor matrix A_0 which in turn is used to compute Ξ_j(component of B_j, see eq. 29) , Δ_j and Λ_j (eq. 30) by appropriately factoring the above tridiagonal matrix. We get for all $1 \leq j \leq J$:

$$Q_0 = A_0$$

so that
$$\Xi_j Q_{j-1} = B_j$$
$$Q_j = A_j - \Xi_j C_{j-1} \qquad (29)$$

and
$$\Lambda_0 = r_0$$
$$\Lambda_j = r_j - \Xi_j \Lambda_{j-1} \qquad (30)$$

In backward sweep we make use of the conditions at the edge of the boundary layer, $\delta F_J = 0$ and $\delta g_J = 0$ that is;

$$Q_J \Delta_J = \Lambda_J$$

and for all $1 \leq j \leq J-1$, $\quad Q_j \Delta_j = \Lambda_j - C_j \Delta_{j+1}$. (31)

An efficient algorithm was written up to compute Δ for a 5 X 5 tridiagonal matrix system using the block elimination method.

Once an appropriate value for the eddy viscosity is introduced into the terms of the finite difference equations containing b, d and e, the elements of the matrix Δ can then be computed. An

iterative process based on Newton's method is applied to reach convergence. Convergence is assumed to have occurred when the following two relationships are satisfied.

$$\left|\frac{\delta G_w}{(G_w+1/2\delta G_w)}\right| \le 0.02, \qquad G(freestream) \le 0.001 \tag{32}$$

where $G = F'$.

4. Extended Mixing Length (Cebeci-Smith)[1] Method

The Cebeci-Smith method as an extended algebraic form of the basic mixing length method has enjoyed a widespread usage in boundary layer calculations. The expressions used in this model are of empirical nature. It is one of the methods which is used in the present work for comparison purposes.

The eddy viscosity in the inner region of the boundary layer is defined by the expression:

$$(\nu_t)_{inner} = l^2 |\partial u/\partial y| \tag{33}$$

where the mixing length l in this equation is given by

$$l = \kappa y \left(1-\exp\left(-\frac{y}{A}\right)\right), \tag{34}$$

and where the constant $\kappa=0.4$ and the damping length constant A is given by the relationship

$$A = 26 \frac{\nu}{N u_\tau^{-1}}. \tag{35}$$

The factor N which controls the effects due to transpiration and pressure gradient is given by,

$$N = \left[\frac{\mu}{\mu_e}\left(\frac{\rho_e}{\rho_w}\right)^2 \frac{p^+}{v_w^+}\left[1-\exp\left(11.8\frac{\mu_w}{\mu}v_w^+\right)\right] + \left(11.8\frac{\mu_w}{\mu}v_w^+\right)\right]^{1/2}. \tag{36}$$

where

$$p^+ = \frac{\nu u_e}{u_\tau^3}\frac{du_e}{dx}, \text{ and } \quad v_w^+ = \frac{v_w}{u_\tau} \tag{37}$$

For flows with no mass transfer a simpler expression for N is used;

$$N = [1 - 11.8\frac{\mu_w}{\mu_e}(\frac{\rho_e}{\rho_w})^2 p^+]^{1/2} \tag{38}$$

For flows with no mass transfer or pressure gradient N = 1.

Another empirical relationship defining an intermittency factor γ_{tr} is used to describe the region of transition to turbulent flow. The equation is

$$\gamma_{tr} = 1 - \exp(-G(x - x_{tr})\int_{x_{tr}}^{x}\frac{dx}{u_e}) \tag{39}$$

x_{tr} refers to the transition location which must be identified and the factor G is given by:

$$G = 8.33 \times 10^{-4}\ u_e^3\ R_x^{-1.34}/\nu^2 \tag{40}$$

In the outer region the following formula is used for the eddy viscosity:

$$(\nu_t)_{outer} = \alpha\left|\int_0^\infty (u_e - u)\,dy\right|\gamma_{tr}\gamma \tag{41}$$

The factor α, for flows with $R_\theta \geq 5000$ is equal to 0.0168. A different expression [18] is used for flows with $R_\theta \leq 5000$. γ is another intermittency factor ($\gamma = 1/(1+5.5(y/y_0)^6)$) representing the intermittent nature of the turbulent flow at the edge of the boundary layer. At the junction of the inner and outer regions of the boundary layer $\nu_{inner} = \nu_{outer}$.

5. The K-e Turbulence Model

The turbulent kinetic energy and the dissipation length balance equations may be expressed in the form (see Reference 20):

$$\rho u\frac{\partial k}{\partial x}+\rho v\frac{\partial k}{\partial y}=\rho\nu_t\left(\frac{\partial u}{\partial y}\right)^2-\rho c_k k\frac{\partial u}{\partial x}-\rho\epsilon+\rho\frac{\partial}{\partial y}\left(\nu_t\frac{\partial k}{\partial y}\right) \tag{42}$$

$$\rho u\frac{\partial \epsilon}{\partial x}+\rho v\frac{\partial \epsilon}{\partial y}=c_1\rho\nu_t\frac{\epsilon}{k}\left(\frac{\partial u}{\partial y}\right)^2-c_3c_k\rho\epsilon\frac{\partial u}{\partial x}-c_2\rho\frac{\epsilon^2}{k}+\rho\frac{\partial}{\partial y}\left(\nu_t\frac{\partial \epsilon}{\partial y}\right) \tag{43}$$

where $\nu_t=c_\mu\frac{k^2}{\epsilon}$ (44)

The equations describing the boundary conditions of the solution are obtained by applying the physical flow conditions at the wall and the edge of the boundary layer:

At the wall $y = y_w$,

$$\epsilon=\frac{\tau^3}{\kappa y}, \qquad \epsilon=c_\mu\frac{k^2}{\epsilon}\left(\frac{\partial u}{\partial y}\right)^2-c_k k\frac{\partial u}{\partial x} \tag{45}$$

At $y = y_{edge}$, $u = u_e$

$$u\frac{\partial k}{\partial x}+\epsilon+c_k k\frac{du_e}{dx}=0 \tag{46}$$

$$u\frac{\partial \epsilon}{\partial x}+c_2\frac{\epsilon^2}{k}+c_3c_k\epsilon\frac{du_e}{dx}=0 \tag{47}$$

Now using the transformation variables as defined in equations 9 and 10, and making use of the non dimensionalizing relationships:

$$\bar{k}=\frac{k}{u_e^2} \quad , \qquad \bar{\epsilon}=\frac{c\epsilon}{u_e^3} \tag{48}$$

The resulting equations are:

$$(\lambda\overline{k'})'+m_1 f\overline{k'}-2m_2\overline{k}F-c_k\overline{k}\left(x\frac{\partial F}{\partial x}+m_2F\right)+\lambda G^2-\overline{\epsilon}x=x\left(F\frac{\partial\overline{k}}{\partial x}-\overline{k'}\frac{\partial f}{\partial x}\right) \qquad (49)$$

$$(\lambda\overline{\epsilon'})'+m_1 f\overline{\epsilon'}-3m_2\overline{\epsilon}F+c_1\lambda G^2\frac{\overline{\epsilon}}{\overline{k}}-c_3c_k\overline{\epsilon}\left(x\frac{\partial F}{\partial x}+m_2F\right)-c_2\frac{\overline{\epsilon^2}}{\overline{k}}x=x\left(F\frac{\partial\overline{\epsilon}}{\partial x}-\overline{\epsilon'}\frac{\partial f}{\partial x}\right) \qquad (50)$$

where once again the normal gradients may be expressed as additional unknowns; i.e.

$$\overline{k'}=K \quad ,\overline{\epsilon'}=E \qquad (51)$$

In the flow field where the eddy viscosity needs to be determined from the k-ϵ equations it must be understood that variables f, $F(=f')$ and $G(=F')$ have already been determined from the earlier solution of the continuity, momentum and energy equations and thus can be introduced in the preceding k-ϵ equations as known quantities. The eddy viscosity ν_t, obtained from the k-ϵ solution, is then used in the boundary layer equations. The cycle is repeated until the convergence criteria stated in equation 32 are satisfied.

As before equations 49 to 51 can be expressed in finite difference form. Incremental coefficients i.e. (k+δk, ϵ+δϵ,K+δK and E+δE) are then introduced in the finite difference formulation so that Newtonian iteration procedure can be applied in conjunction with Keller's box method.

In vector notation then for the four equations we can write:

$$[\underline{L}]\underline{\Delta} = \underline{R} \qquad (52)$$

Here $\underline{L}$ represents a 4 X 4 matrix containing the coefficients of the unknowns $\underline{\Delta}$ (δk, δϵ.,δK and δE) and the right hand $\underline{R}$ side contains all of the remaining terms. To use the block elimination method the equation is rewritten with the matrix $\underline{L}$ expressed in a tridiagonal format with end matrices conforming to the boundary conditions. Thus as before we have

$$\begin{vmatrix} \alpha_0\gamma_0 & & \\ \beta_j\alpha_j\gamma_j & & \\ & \beta_J\alpha_J & \end{vmatrix} \begin{vmatrix} \\ \Delta \\ \\ \end{vmatrix} = \begin{vmatrix} \\ \underline{R} \\ \\ \end{vmatrix} \qquad (53)$$

Matrices α_0, γ_0 and α_J, γ_J are obtained from the finite difference equations describing the wall and the edge conditions of the boundary layer. The definitions of α_j, β_j and γ_j of course correspond to those for B_j, A_j and C_j in section 2. An algorithm (mentioned earlier) written for the solution of 5 X 5 tridiagonal matrix system, was used again with a small modification to solve Δ for the present 4 X 4 tridiagonal matrix system. .

The above k-ϵ method is applied to the outer boundary layer region $y^+ \geq 60$. For the inner part of the boundary layer the Cebeci-Smith extended mixing length model is used . The solutions at the match point make use of the wall functions which relate the flow quantities at the first grid point to the shear stress τ_w or the friction velocity $u_\tau = \sqrt{(\tau_w/\rho)}$. At the first grid point the turbulence is assumed to be in local equilibrium which along with other assumptions of the mixing length model provide the starting k and ϵ values. Thus as in Ref [21] we have:

$$k_1 = \frac{u^2_\tau}{\sqrt{c_\mu}} \quad , \quad \epsilon_1 = \frac{u^3_\tau}{\kappa y_1} \tag{54}$$

To initiate the iterative process we need to define the complete k and ϵ profiles which can be generated by the use of a shear stress profile which from Ref [22] is given by:

$$\frac{\tau}{\tau_w} = 1 + \frac{\delta}{\theta}\left(\int_0^\zeta F^2 d\zeta - F\int_0^\zeta F d\zeta\right) - \frac{2}{c_f}\frac{\delta}{u_e}\frac{du_e}{dx}\left[\zeta - F\int_0^\zeta F d\zeta + \frac{\delta^*}{\theta}\left(\int_0^\zeta F^2 d\zeta - F\int_0^\zeta F d\zeta\right)\right] \tag{55}$$

where as in Ref [22] it is assumed that $u = u_e F(\zeta)$, δ/θ=constant and $\zeta = y/\delta$. Furthermore, the extended mixing length model may be used for determining the initial τ_w, c_f, δ, δ^*, and θ values. The formulae used for obtaining the first k and ϵ profiles are then given by $k = 1/0.3\tau$ and $\epsilon = \tau\, \partial u/\partial y$, or alternatively, the ϵ profile may be determined from the relationship $\nu_t = c_\mu k^2/\epsilon$ if the eddy viscosity profile is known.

The iteration cycle within this model is repeated until the resultant eddy viscosity $\left(\nu_t = c_\mu \frac{k^2}{\epsilon}\right)$ computed from the current values of k and ϵ is such that it enables the boundary layer equations (eq.4 to 6) in section 3 to converge.

6. Discussion of Results

Generally it was found that the Cebeci-Smith extended mixing length model would converge in up to 4 iterations. The k-ϵ model in some cases took 1 to 2 extra iterations to converge. Since we are solving 4 (two main k and ϵ, plus two normal gradient equations) extra equations within a separate iterative module which in turn feeds the main program solving the momentum and energy equations, the k-ϵ method takes more than double the CPU time of the Cebeci-Smith method which is consistent with the findings in Ref [23]. For the purposes of this investigation a number of cases were selected from the literature and appropriate comparisons were made for such boundary layer parameters as c_f, δ^*, H, u/u_e and θ.

Figures 2 to 5 show boundary layer computations of skin friction coefficient c_f, velocity distribution u/u_e and shear stress τ profile across the boundary layer formed on the inside surface of a cylindrical body. Where the experimental data are available it is shown for comparison. This experiment [24] reported as Case 7201 in Ref [5] was specially designed to show the effects of pressure gradient and compressibility. The tests were performed on the inner surface of a cylinder which was centrally mounted inside the wind tunnel. Another centre body was used for imposing various pressure gradients. The outer shell had an inside diameter of 20 inches and a length of 50 inches. The bondary layer generated on the inside surface of the cylindrical body was free from end effects associated with planar models. With a large constant radius of the cylindrical body ($\delta/r \leq 0.07$), any effects from axially symmetric flow were minimized and those due to streamwise surface curveture were eliminated. The Mach number distribution for which the current computations were carried out is shown in Figure 2.

Both methods have successfully computed the general trend of skin friction distribution as shown in Figure 2. In the upstream regions, $x \leq 14$ in., both methods seem to over-predict the skin friction whilst the converse is generally true for regions $x \geq 18$ in. Or judging by the location of the shock wave, the computed results in the axial direction seem to be out of phase by about 1 in.

Figures 3, 4 and 5 show velocity profiles and shear stress comparisons at axial stations 11.5, 16.0 and 21.5 inches respectively. Whilst the comparison between the two methods seems to be very good, both methods show poor velocity distribution comparison with experiment at $x = 11.5$ in., for $y/\theta \leq 10$. At $x = 16$ in., both methods show good velocity profile comparison against the measure data. At $x = 21.5$ in., again the comparison is poor for $y/\theta \leq 7.5$. In this case some discrepancy is expected as the computations from a 2D code are being compared against measurement conducted in an axisymmetric internal flow.

There was no shear stress data available to be compared with computations.

Figures 6 to 10 show comparisons of boundary layer characteristics for a 12 % thick supercritical airfoil with aspect ratio of 3 (case 8621 in Ref [5]), as predicted by the two methods and the measurements.

Figure 6 shows the skin friction distribution comparison at M = 0.725, α = 2.92 deg and Re/c = 6.5 X 10^6 with transition fixed at x/c = 0.03 . The results from the extended mixing length model seem to be follow the k-ϵ predictions closely. On the whole they show satisfactory agreement with the experiment where the measured data are available. Another skin friction comparison for the same airfoil at M = 0.73, α = 3.19 deg and Re/c = 6.5 X 10^6 with transition still fixed at 3 % is provided in Figure 7. The skin friction is over predicted by as much as 0.00029 at some stations.

Figure 8 shows the displacement thickness normalized with respect to chord (δ^*/c) and the form parameter H (δ^*/θ) comparison for the case where M = 0.725 and α = 2.92 deg. For the δ^*/c comparison, both methods predict good agreement with the measured data in the forward portion of the airfoil. In the rearward regions both under predict the δ^*/c values with the k-ϵ results falling relatively closer to the experiment. For the H comparison, in the forward region the k-ϵ results are larger by an amount 0.16 than the experiment. The extended mixing length model gives better agreement of results here. In the rearward region the k-ϵ predictions are closer to the experiment.

Figures 9 and 10 show the velocity distribution and shear stress profiles at stations x/c = 0.325 and 0.9 respectively, for the flow condition identified in Figure 6. The velocity distributions are well predicted by both methods at x/c = 0.325, however, the comparison is not as good at x/c = 0.9. The two methods predict very similar shear stress profiles at both stations.

Figures 11 and 12 show the velocity and shear stress profiles at axial stations x/c = 0.45 and 0.8 for an 11 % thick airfoil with an aspect ratio of 4 tested in the NASA-Ames tunnel. It is referred as case 8623 in Ref [5]. The flow conditions were: M = 0.8 , α = 2.4 deg and Re/c = 3 X 10^6 with the transition fixed at x/c = 0.35. The computations for the velocity distribution seem to sit comfortably amid the experimental results at x/c = 0.45 in Figure 11. Even at x/c = 0.8 both prediction methods seem to give satisfactory results at most regions of the boundary layer. Except for a small kink near the wall in Figure 12 the shear stress trends seem to be very similar as computed by both methods.

Some computations were also carried out to test the applicability of the present methods when the mass flow is injected or removed from the boundary layer. Figure 13 shows the velocity

profile comparison for Squire's [25] flat plate experiment with a flow injection rate of $\rho_w v_w / \rho_e u_e = 0.0013$. Other flow conditions were $M_e = 1.8$, Re/ft = 8 X 10^6 and $T_0 = 293\ ^0C$. The velocity profile at $Re_\theta = 17500$ was obtained by matching the momentum thickness at the first measurement station. A comparison of the displacement thickness δ^* and momentum thickness θ (both normalized with respect to chord c) with measured values at injection rates of 0 and 0.0013 is shown in Figures 14 and 15. In all cases the agreement is encouraging.

7. Conclusions

A general purpose boundary layer computer code has been written with the option to use either the Cebeci-Smith algebraic turbulence model or the k-ϵ turbulence model to effect closure.

It was found that the k-ϵ model which solves the main turbulent kinetic energy and the dissipation energy equations using the standard block reduction method [19] and Newton's convergence approach can be successfully linked to the main program which was originally written to accept the algebraic model [1].

Both methods provide satisfactory agreement with the experimental results reported in literature.

From efficiency and convenience viewpoint the Cebeci-Smith model was found to be more acceptable than the k-ϵ model.

References

1. Cebeci, T and A. M. O. Smith., 'Analysis of Turbulent Boundary Layers,' Academic Press, New York (1974)
2. Jones, W. P. and Launder, B. E., 'The prediction of laminarization with two equation model of turbulence', International Journal of Heat and Mass Transfer, Vol. 15, 1972.
3. Hirsh, R. S., Friedman., D. M. and Cebeci, T., 'Solution of turbulent transport equations by an accurate numerical method,' Lecture Notes in Physics. Sixth International Conference on numerical Methods in Fluid Dynamics, Springer-Verlag, p. 274, 1979.
4. Cebeci, T., and Meier, H. U., 'Modelling requirements for the calculation of the turbulent flow around airfoils, wings and bodies of revolution', AGARD CP 271, Paper 6, 1979.
5. Proceedings of the 1980-1981 AFSOR-HTTM-STANFORD Conference on Complex Turbulent Flows - Editors Kline, S. J., Cantwell, B. J. and Lilley, G. M., Stanford University, Stanford, California.
6. Prandtl, L., 'Ober die ausgebildete Turbulenz,' ZAMM, 5, 1925.
7. Patankar, S. V., and D. B. Spaling, 'Heat and Mass Transfer in Boundary Layers', C.R.C. Press, Cleveland , 1968.
8. Launder, B.E., and C. H. Pridden, ' A comparison of some proposals for the mixing length near a wall, ' International Journal of Heat and Mass Transfer, vol 17, No.2, 1974, pp. 293-306.

9. Kays, W. M., and R. J. Moffat, 'The behaviour of transpired turbulent boundary layers,' "Studies in Convection" Vol. 1, B. E. Launder, ed., Academic Press, London, 1975.
10. van Driest, E. R., 'On turbulent flow near a wall,' Journal of Aeronautical Sciences, Vol.23, 1956 pp. 1007-1011, 1036.
11. McDonald, H and F.J. Camarata, 'An extended mixing length approach for computing the turbulent boundary layer development,' Proceedings computations of turbulent Boundary layers-1968, AFSOR-IFP-Stanford Conference Vol. 1, Aug. 1968, Stanford university., Stanford, Calif., pp. 83-98.
12. Bradshaw, P., D. H. Ferriss., and N. P. Atwell., 'Calculations of boundary layers development using the turbulent energy equation,' Journal of Fluid Mechanics, Vol.28, Pt.3, 1967.
13 Chan., Y. Y., 'Turbulent boundary-layer computations based on an extended mixing length approach,' AIAA Journal, Vol. 8, No. pp. 1873-1875, 1970.
14. Baldwin, B. S. and Lomax, H, 'Thin layer approximations and algebraic models for separated flows,' AIAA Paper 78-257 1978.
15. Lilley., G. M., ' An approximate solution of the turbulent boundary layer equations in incompressible and compressible flow,' The College of Aeronautics Cranfield. Report No. 134 July 1960.
16. Townsend, A. A. 'The structure of turbulent shear flow,' C.U.P., 1956.
17. Hanjalic., K and Launder, B. E., ' A Reynolds stress model of turbulence and its application to thin shear flows,' Journal of Fluid Mechanics, Vol. 52, Part 4, pp. 609-638, 1972.
18. Cebeci, T, and Bradshaw, P, 'Physical and Computational Aspects of Convective Heat Transfer,' Springer-Verlag 1984.
19. Keller, H. B. 'A new differential scheme for parabolic problems. Numerical Solutions of Partial Differential Equations, J. Bramble, ed., vol. II, Academic Press, 1970.
20. Cebeci, T., Chang,K.C., Li, C. and Whitelaw, J. H, 'Turbulence models for wall boundary layers', California State University, Report ME-84-2, August 1984.
21. Introduction to the modelling of turbulence. A short course at von Karman Institute for Fluid Dynamics. 1985-01
22. Cebeci, T., Chang, K.C. and Bradshaw, P, 'Solution of a hyperbolic system of turbulence-model equations by the "box" method,' Computer Methods in Applied Mechanics and Engineering Vol.22 1980. North-Holland publishing Company.
23. Cebeci, T., Chang, K.C., Li, C. and Whitelaw, J. H., 'Turbulence models for wall boundary laters,' AIAA Journal, Vol. 24, No. 3, 1986.
24. Lewis, J. E., Gran, R. L. and Kubota, T., 'An experiment in the adiabatic compressible turbulent boundary layer in adverse and favourable pressure gradient. Journal of Fluid Mechanics, Vol. 51 1972.
25. Squire, L. C., 'Further Experimental Investigation of Compressible Turbulent Boudary Layers with Air Injection', A.R.C.R. & M. No.3627 August 1968.

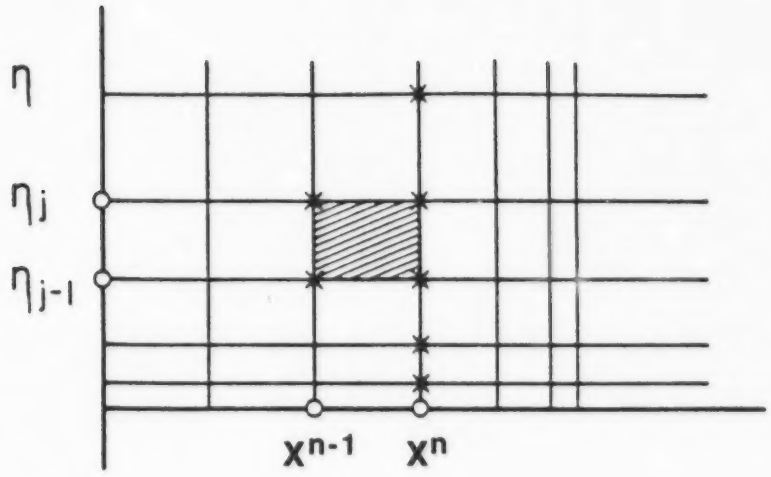

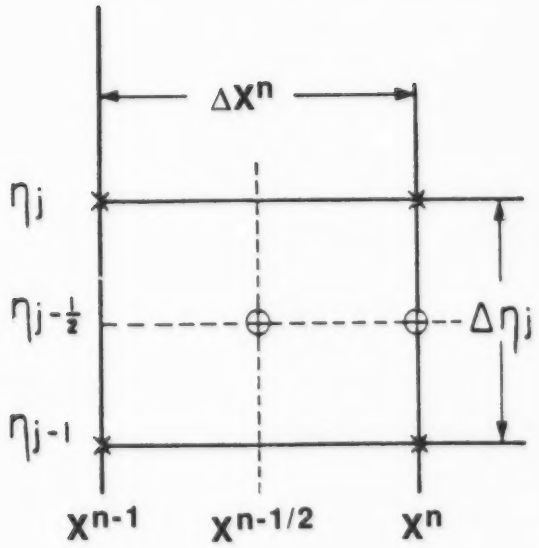

FIG. 1: GRID RECTANGLE FOR THE FINITE DIFFERENCE SCHEME

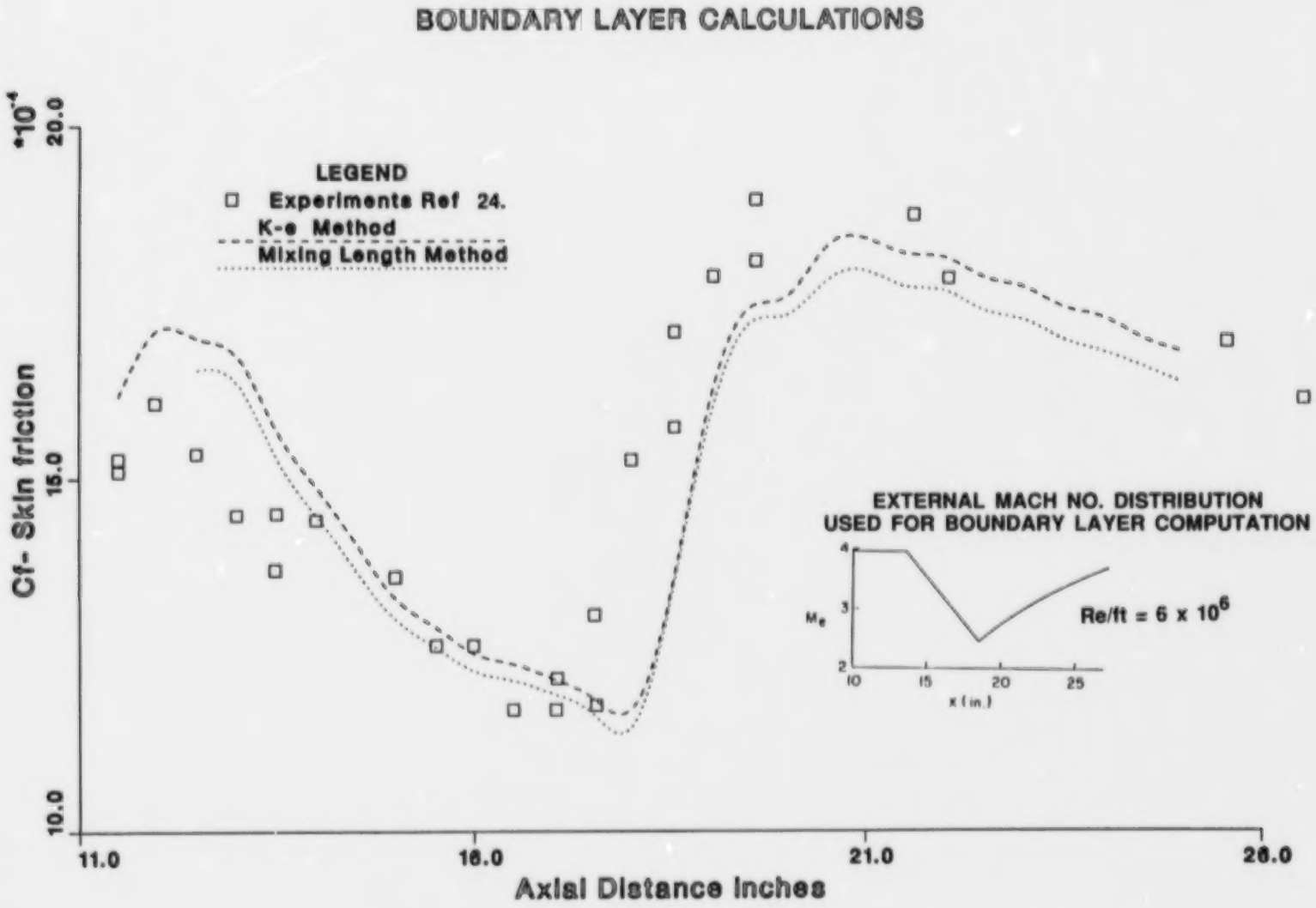

FIG. 2: SKIN-FRICTION COEFFICIENT C_f versus AXIAL DISTANCE

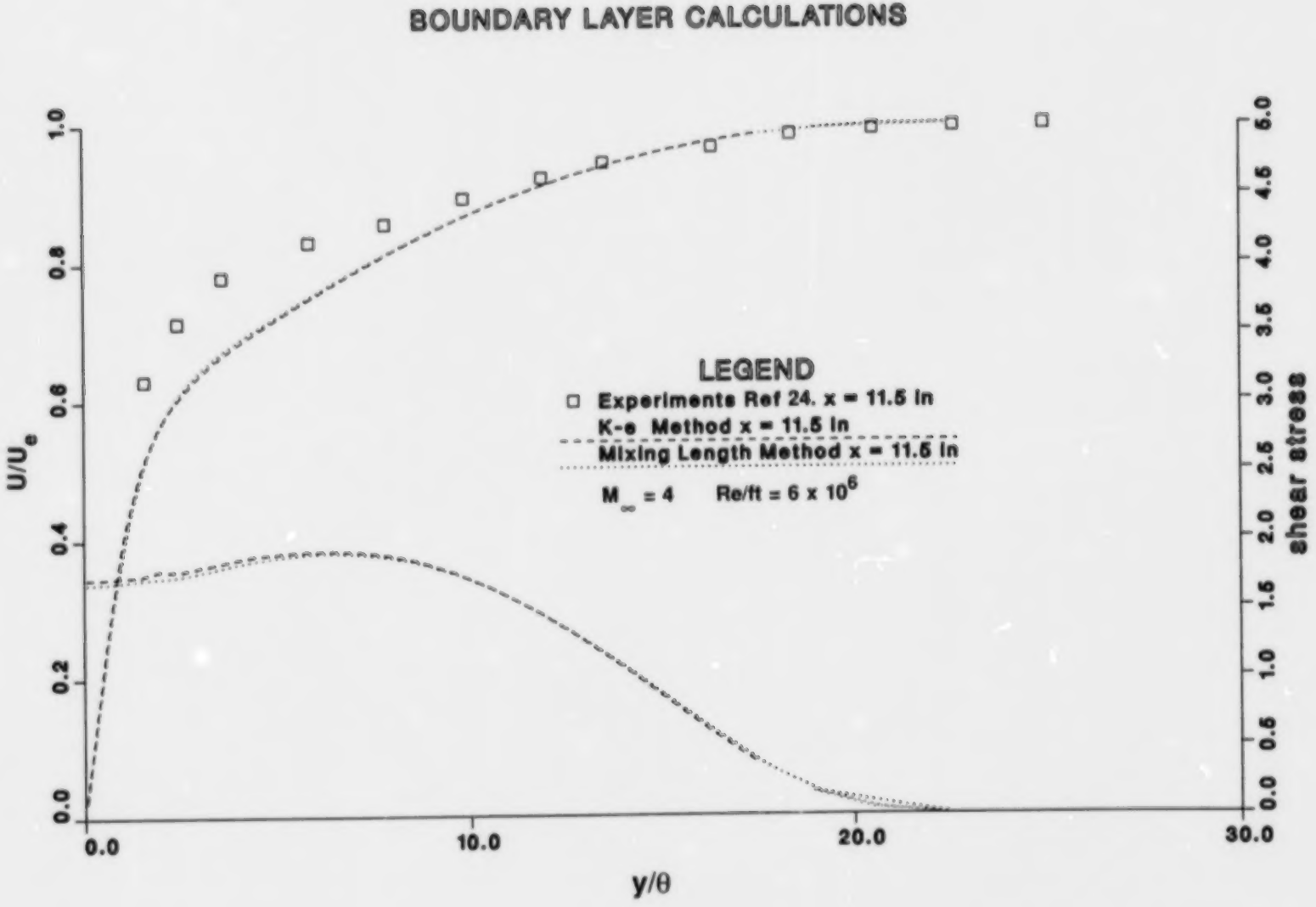

FIG. 3: VELOCITY U/U_e AND SHEAR STRESS τ PROFILES ACROSS BOUNDARY LAYER

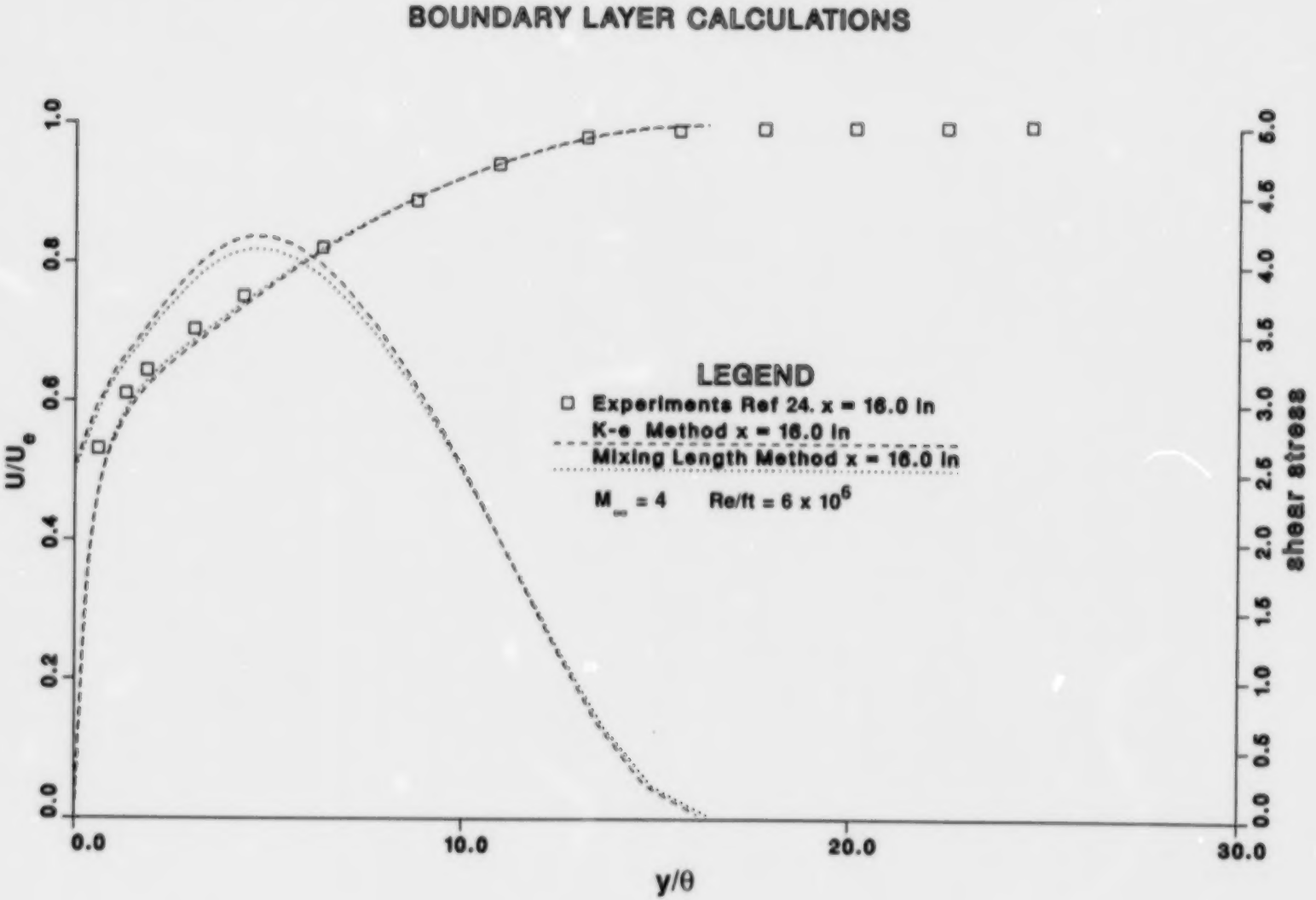

FIG. 4: VELOCITY U/U_e AND SHEAR STRESS τ PROFILES ACROSS BOUNDARY LAYER

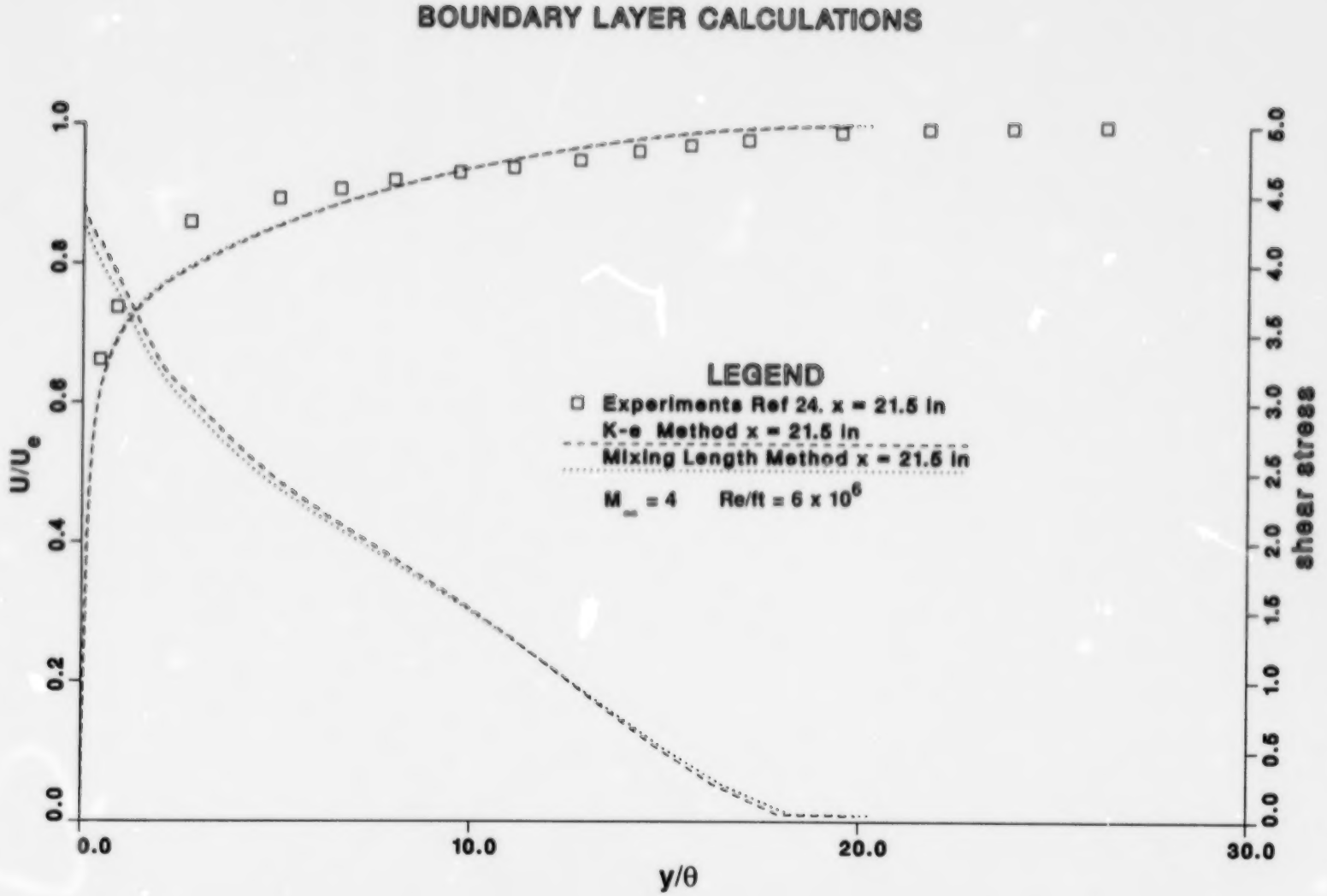

FIG. 5: VELOCITY U/U_e AND SHEAR STRESS τ PROFILES ACROSS BOUNDARY LAYER

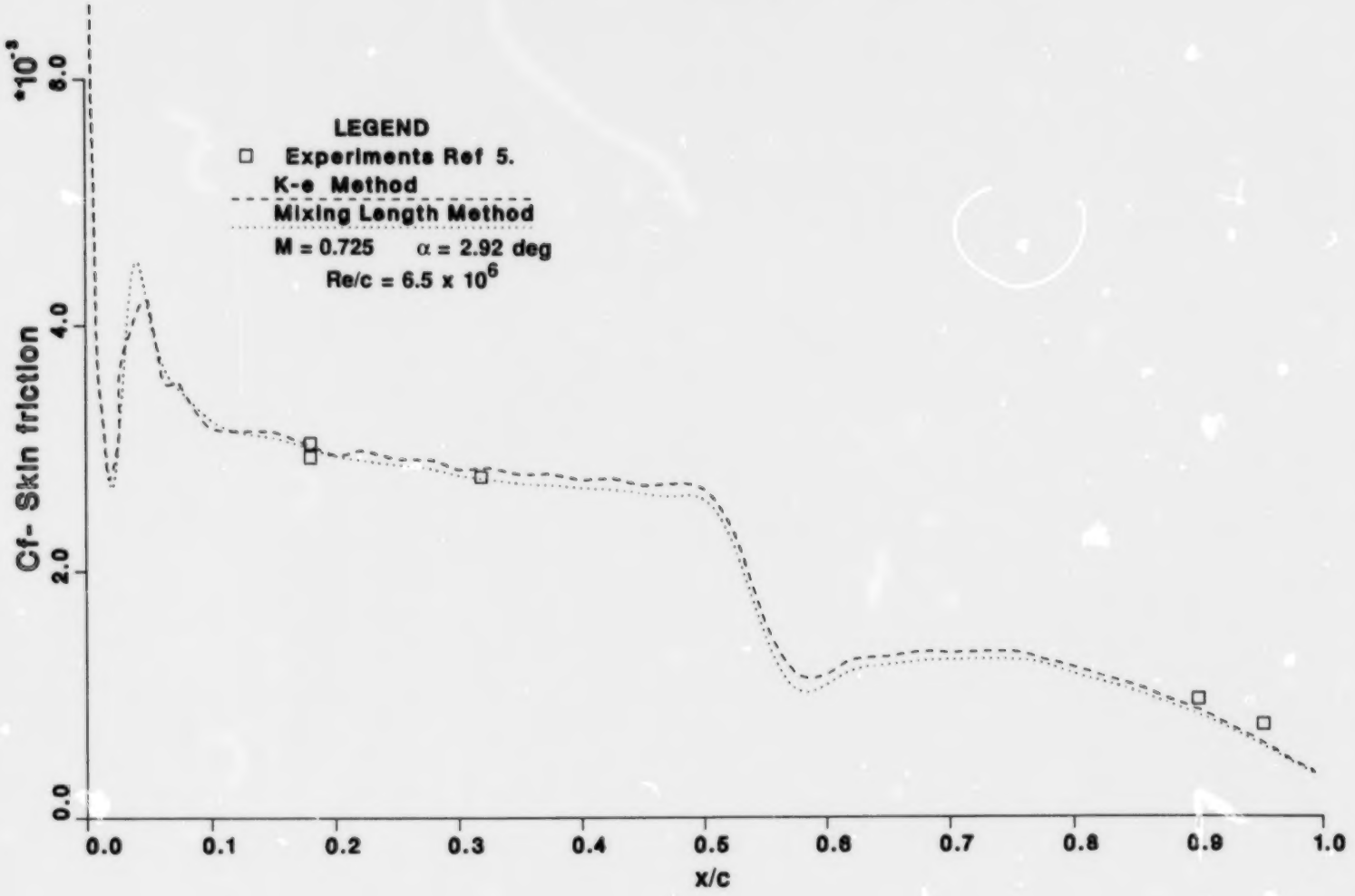

FIG. 6: SKIN FRICTION COEFFICIENT C_f versus x/c

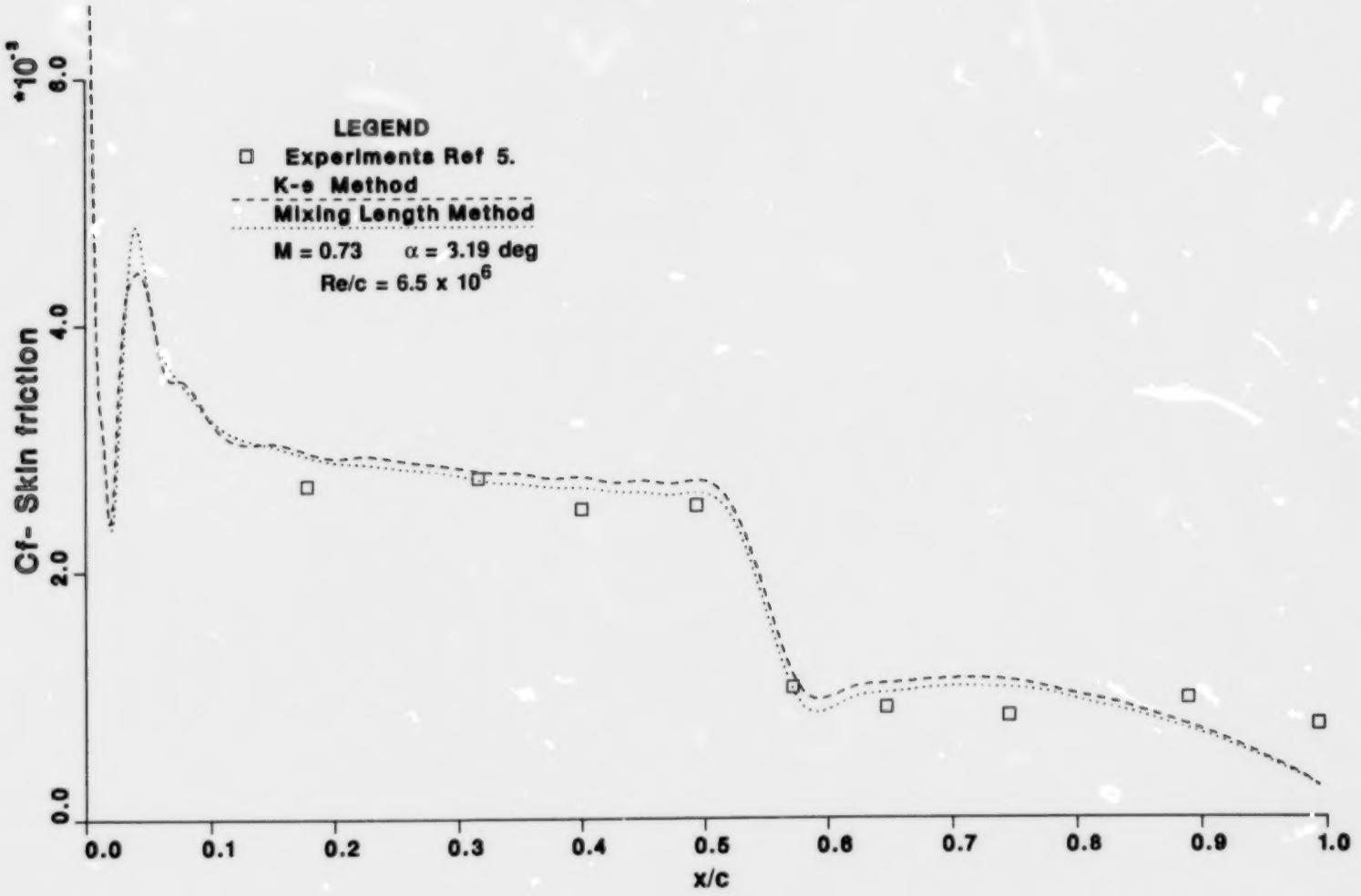

FIG. 7: SKIN FRICTION COEFFICIENT C_f versus x/c

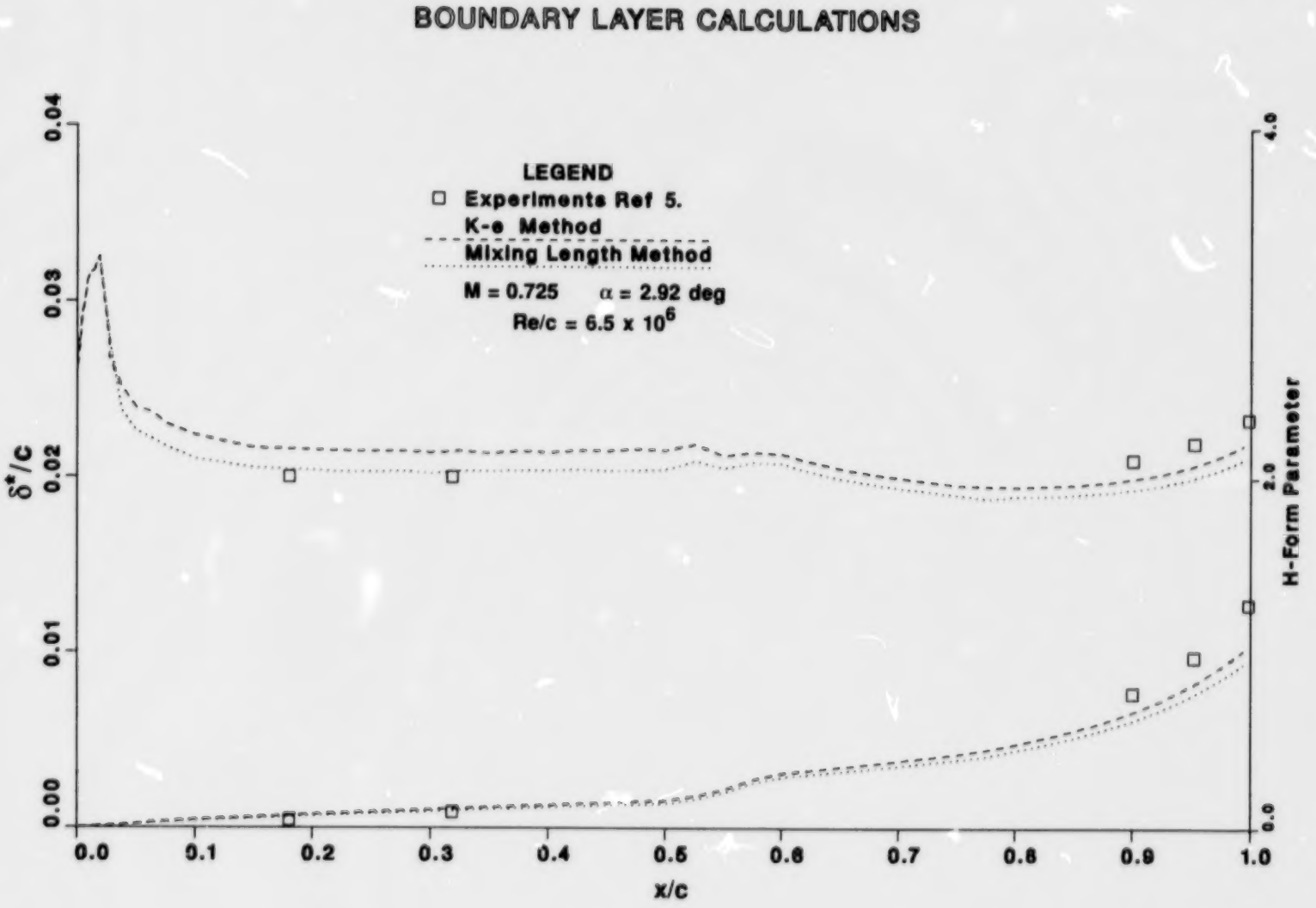

FIG. 8: DISPLACEMENT THICKNESS δ^* AND FORM PARAMETER H versus x/c

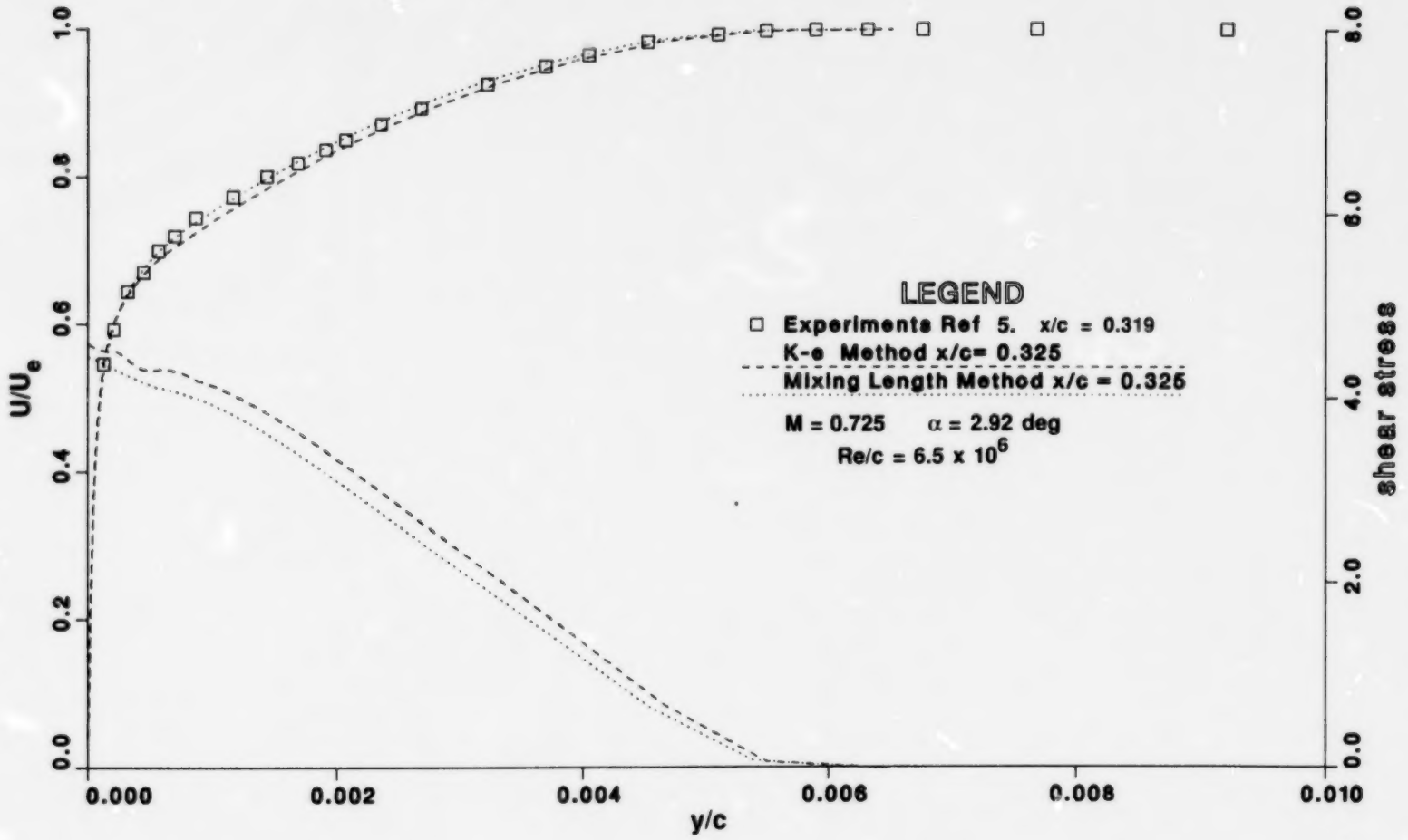

FIG. 9: VELOCITY U/U_e AND SHEAR STRESS τ PROFILES ACROSS BOUNDARY LAYER

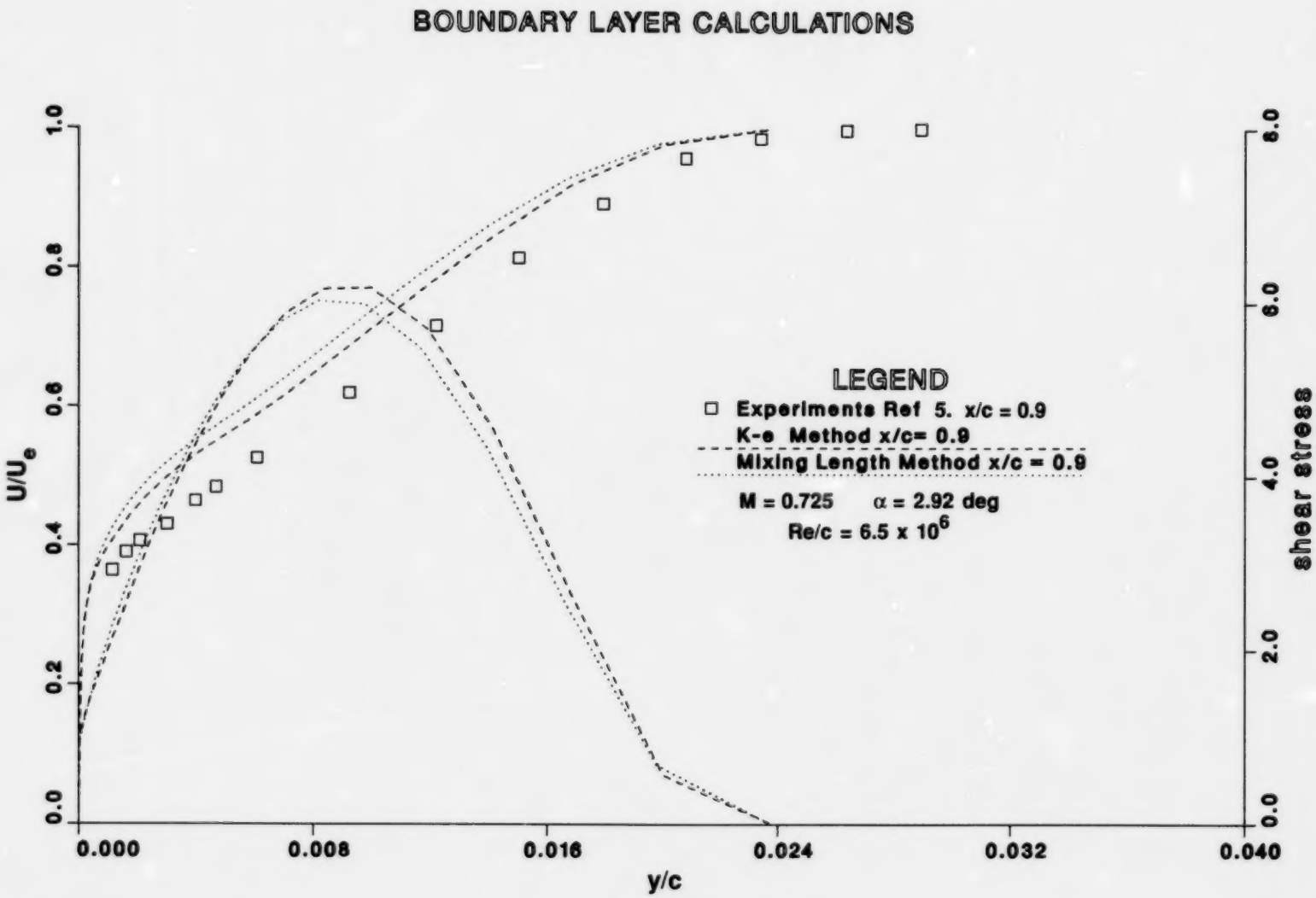

FIG. 10: VELOCITY U/U_e AND SHEAR STRESS τ PROFILES ACROSS BOUNDARY LAYER

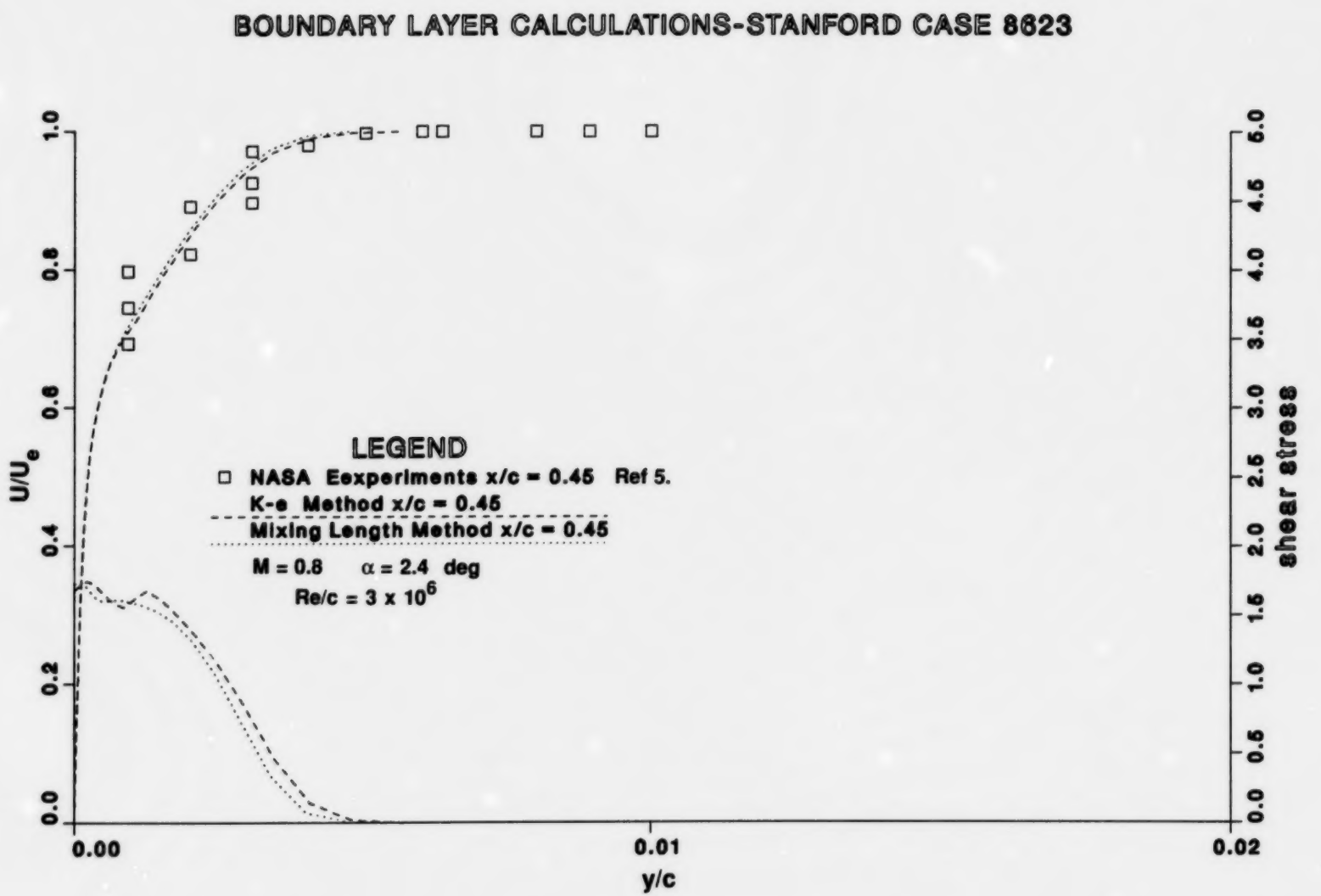

FIG. 11: VELOCITY U/U_e AND SHEAR STRESS τ PROFILES ACROSS BOUNDARY LAYER

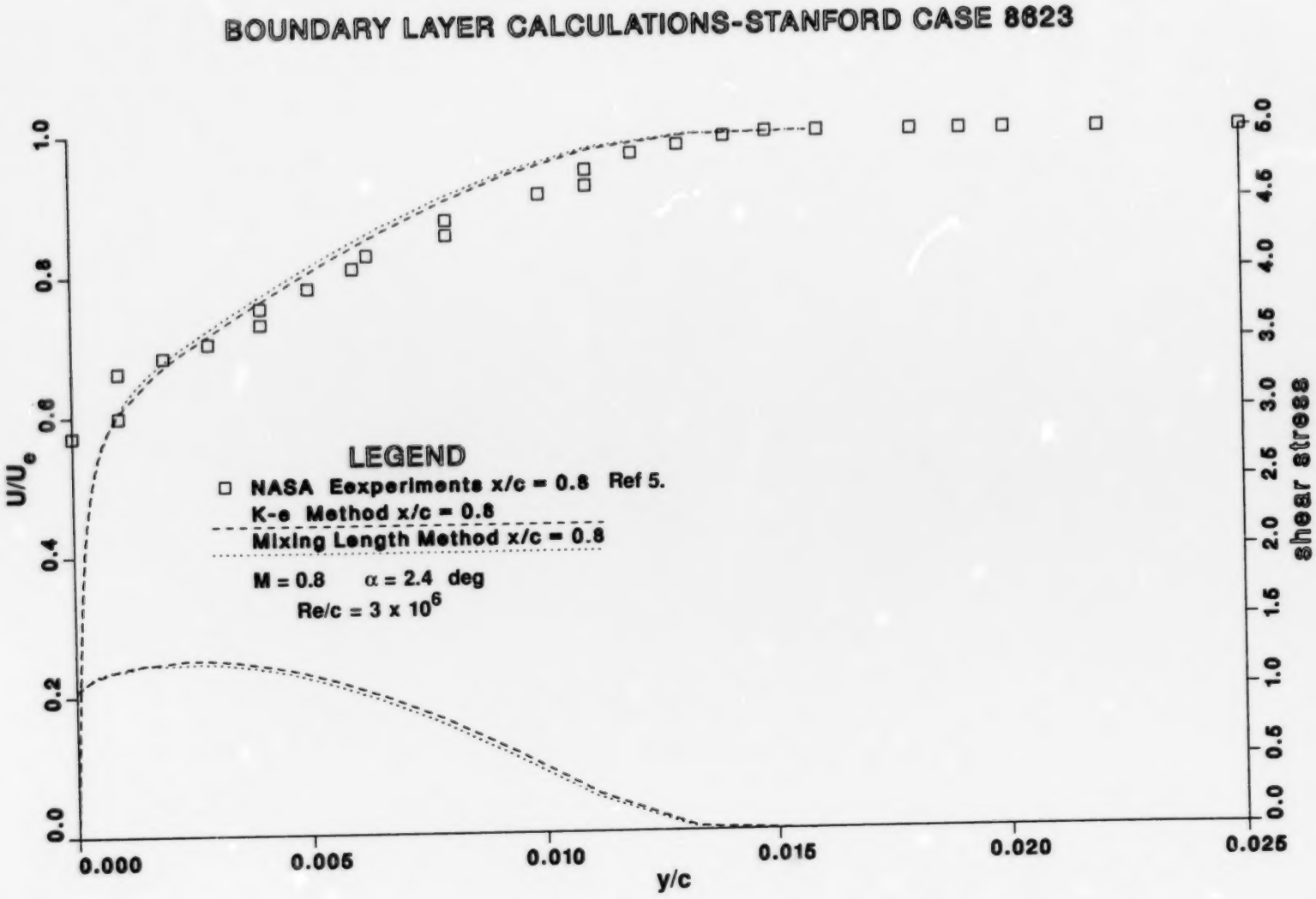

FIG. 12: VELOCITY U/U_e AND SHEAR STRESS τ PROFILES ACROSS BOUNDARY LAYER

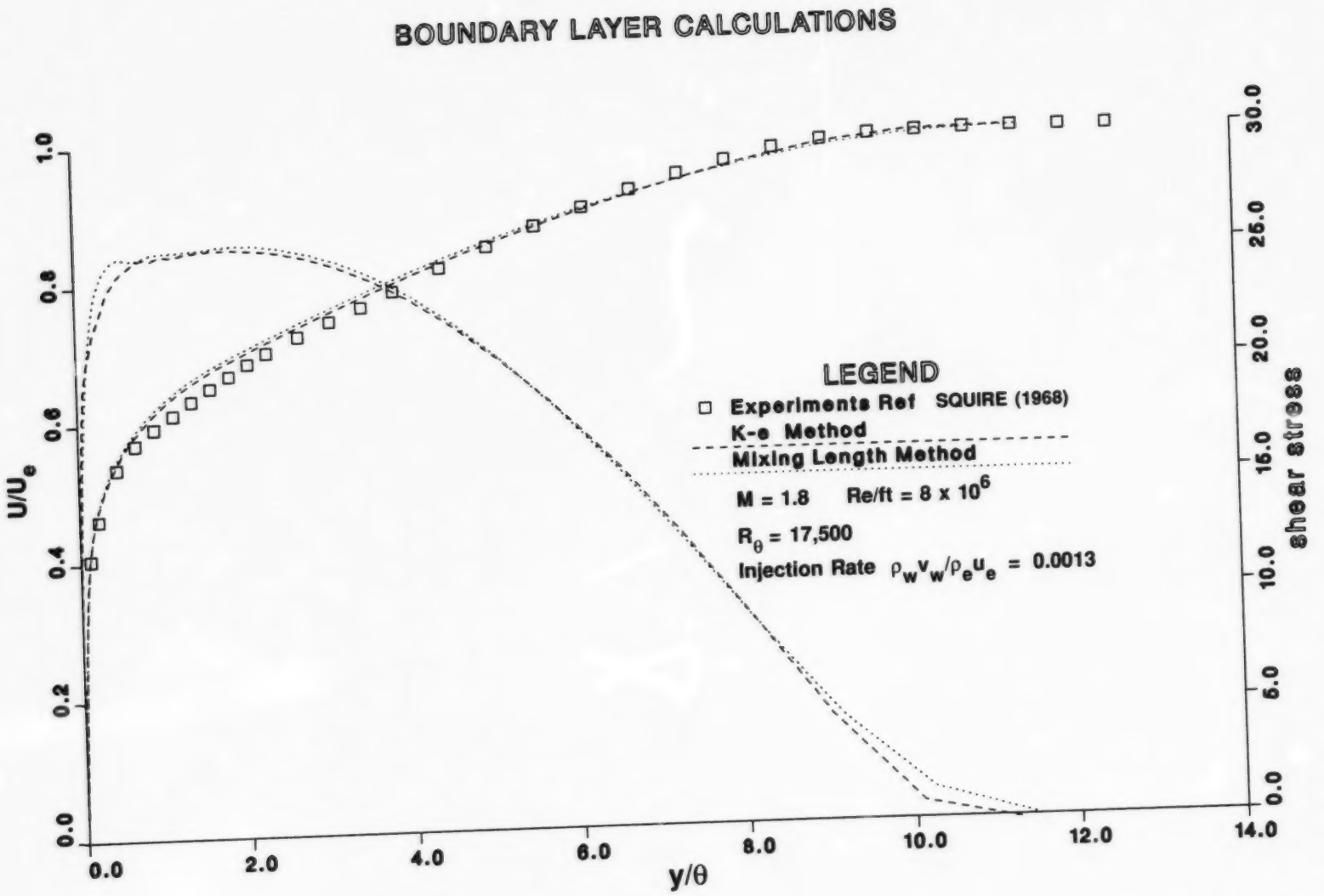

FIG. 13: VELOCITY U/U_e AND SHEAR STRESS τ PROFILES ACROSS BOUNDARY LAYER

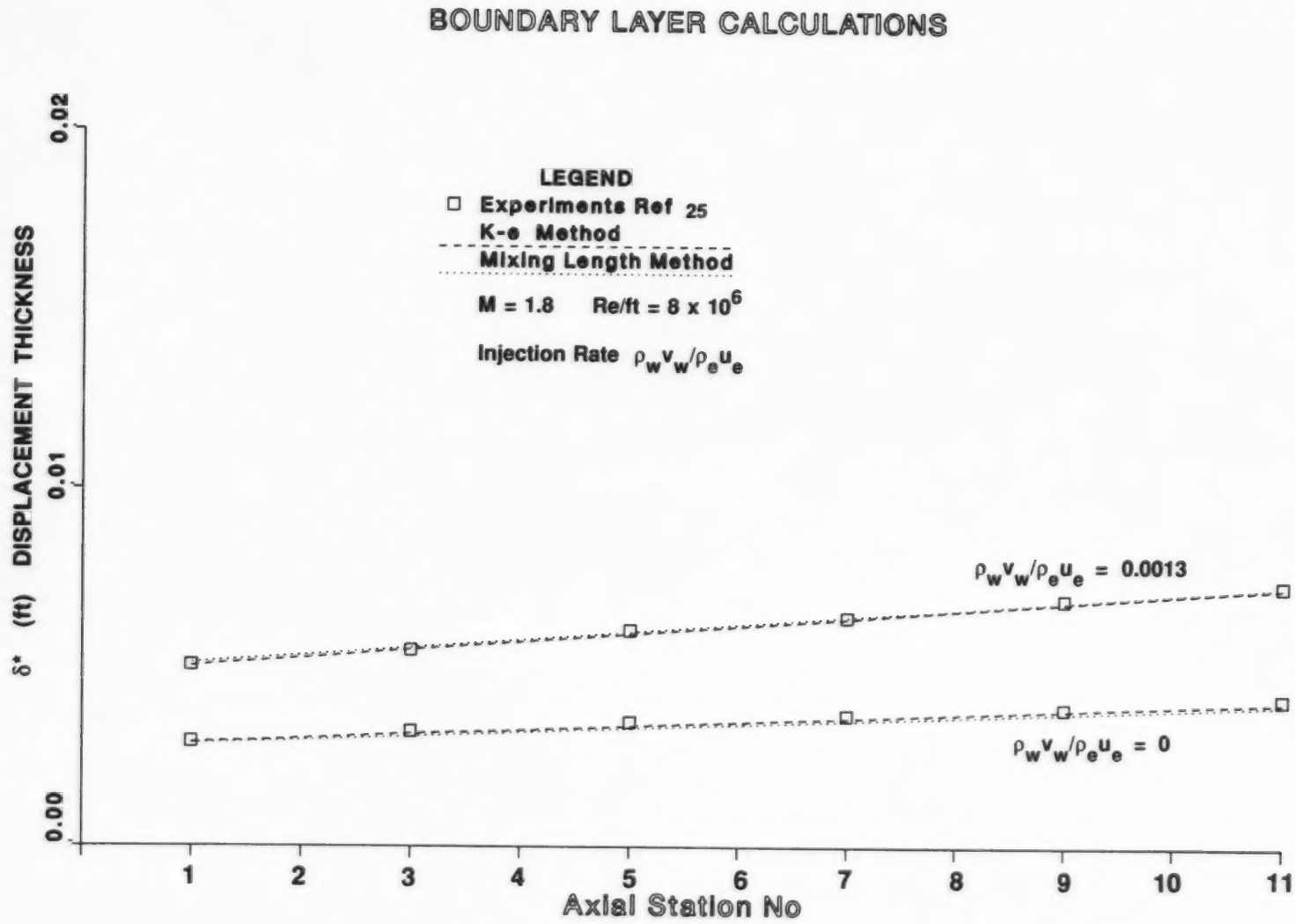

FIG. 14: DISPLACEMENT THICKNESS δ^* versus AXIAL STATION

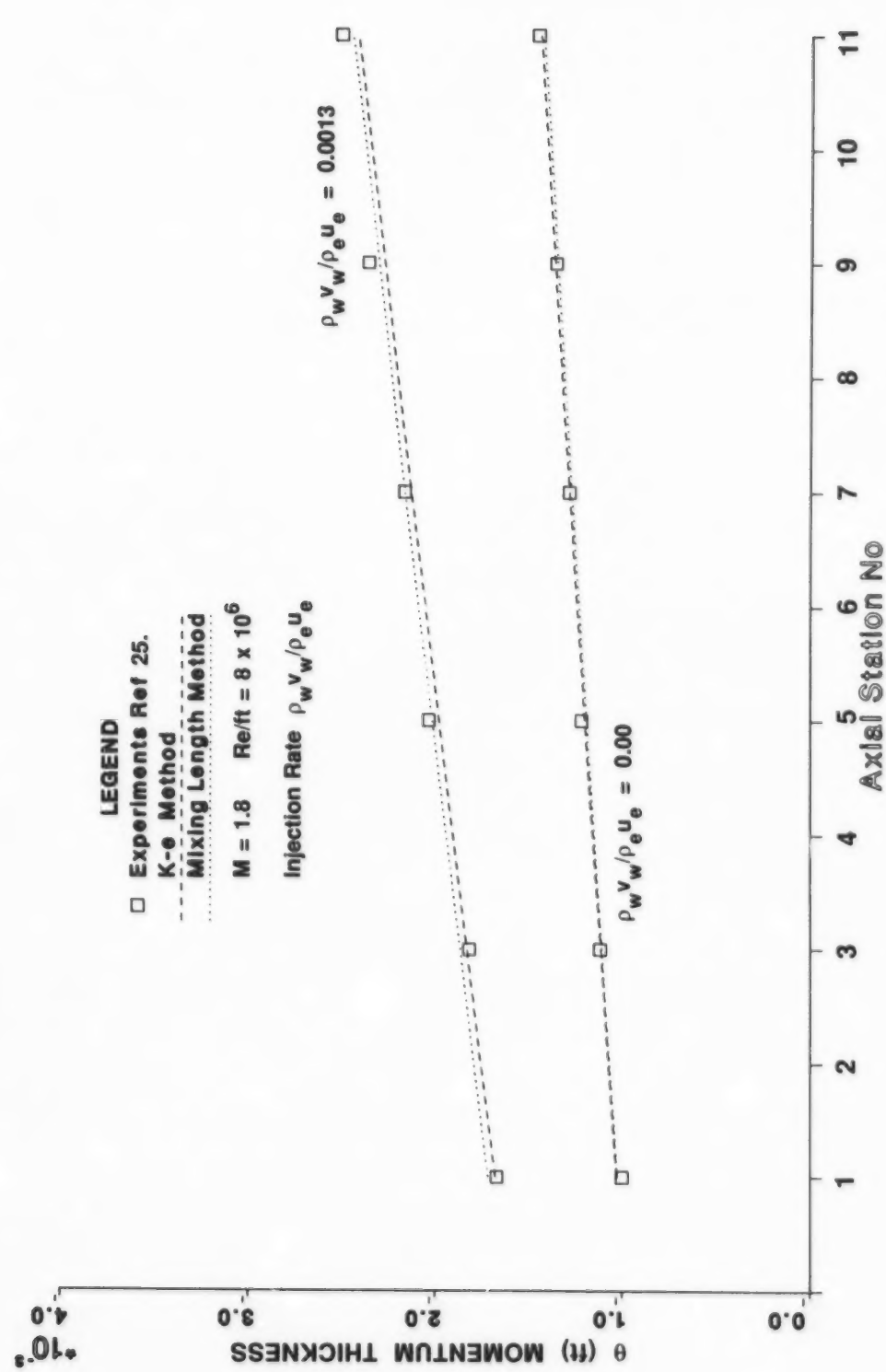

FIG. 15: MOMENTUM THICKNESS θ versus AXIAL STATION

REPORT DOCUMENTATION PAGE / PAGE DE DOCUMENTATION DE RAPPORT

REPORT/RAPPORT 1a	REPORT/RAPPORT 1b
IAR-AN-69	NRC No. 32135
REPORT SECURITY CLASSIFICATION CLASSIFICATION DE SÉCURITÉ DE RAPPORT 2	DISTRIBUTION (LIMITATIONS) 3
Unclassified	Unlimited

TITLE/SUBTITLE/TITRE/SOUS-TITRE
4

Turbulent Boundary Layer Solution for Two-Dimensional Compressible Flow Using Mixing Length For K-ε Turbulence Models

AUTHOR(S)/AUTEUR(S)
5

M. Khalid

SERIES/SÉRIE
6

Aeronautical Note

CORPORATE AUTHOR/PERFORMING AGENCY/AUTEUR D'ENTREPRISE/AGENCE D'EXÉCUTION
7

National Research Council Canada
Institute for Aerospace Research

High Speed Aerodynamics Lboratory

SPONSORING AGENCY/AGENCE DE SUBVENTION
8

DATE 9	FILE/DOSSIER 10	LAB. ORDER COMMANDE DE LAB. 11	PAGES 12a	FIGS./DIAGRAMMES 12b
11-90			31	15

NOTES
13

DESCRIPTORS (KEY WORDS)/MOTS-CLÉS
14

1. Turbulent Boundary Layer
2. Compressible Boundary Layer
3. Two Dimensional Bounday Layer

SUMMARY/SOMMAIRE

The continuity, momentum and energy equations for two-dimensional compressible turublent boundary layers are solved using the k-ε turbulence model and the extended mixing length approach to calculate the shear stress terms. The finite difference equations are set up applying Keller's box scheme and the resulting tridiagonal matrix system is solved by the block elimination method. Newton's iteration procedure is used to converge the solution. Results obtained from computations showed only slight difference between the two methods. Both methods showed satisfactory agreement with experimental data for test cases.

15